J Appl Electrochem (2012) 42:111–120
DOI 10.1007/s10800-011-0377-x

ORIGINAL PAPER

In situ infrared attenuated total reflectance spectroelectrochemical study of lubricant degradation

Bushan K. Purushothaman · Michael Pelsozy · Philip W. Morrison Jr. · Vadim F. Lvovich · Heidi B. Martin

Received: 7 October 2011 / Accepted: 30 December 2011 / Published online: 10 January 2012

Abstract An attenuated total reflectance (ATR) infrared (IR) cell was designed using a boron-doped silicon wafer as the optically transparent electrode to simultaneously perform ATR-IR spectroscopic and electrochemical impedance measurements. The degradation of industrial lubricants was investigated by monitoring the near-surface concentration of hydrocarbons, detergents and anti-wear additives and the formation of degradation products, while polarizing the cell using electrochemical impedance spectroscopy (EIS). The detergent and the anti-wear agent concentration on and near the silicon surface, based on the IR spectra, and the sum of bulk solution and charge transfer resistance, based on the impedance spectra, were all at a maximum for 30 h drain oil, and then decreased for later drain oils. These results agree with other independent measurements, such as oil viscosity, total acid number (TAN), and total base number (TBN) to indicate that the lubricant is significantly degraded after 30 h in the engine test. These data demonstrate the potential use of the ATR silicon-based electrochemical cell as a monitoring device for lubricant degradation, and as an effective analytical tool capable of studying interfacial kinetics, surface interactions of the additives, and performance of silicon-based spectroelectrochemical devices.

Keywords Spectroelectrochemical · Attenuated total reflectance · Lubricant degradation · Boron doped silicon · Optically transparent electrode

1 Introduction

Attenuated total reflectance (ATR) spectroscopy is a well-developed in situ technique to quantitatively explore chemical interactions at solid–fluid (liquid or gas) interfaces; e.g., species adsorption/desorption and kinetics and mechanisms of surface reactions [1, 2]. In comparison to other spectroscopy measurement geometries (i.e., transmission or external reflection), ATR spectroscopy has advantage of a short effective path length into the fluid and thus probes only the near-interface region. Spectroelectrochemistry, i.e., coupled spectroscopic and electrochemical measurement, provides additional molecular insight into electrochemical reactions at the electrode surface [3, 4]. The solution layer thickness is not limited in the ATR geometry making it more suitable for spectroelectrochemical measurements and also facilitating uniform current density distribution on the electrode surface. However, for ATR spectroelectrochemistry in Kretschmann configuration, optically transparent electrodes are necessary; and, very few materials are both optically transparent in the IR and electrically conductive. Most ATR spectroelectrochemical applications utilize a thin metal film deposited onto an internal reflection element (IRE) as the optically transparent electrode [5, 6].

Dedication The authors wish to dedicate this paper to the late Professor Philip W. Morrison, Jr. (1960–2002). We honor his innovation and intellect as a scientist and engineer, and his compassion for his research and students.

B. K. Purushothaman (✉) · M. Pelsozy · P. W. Morrison Jr. · V. F. Lvovich · H. B. Martin
Department of Chemical Engineering, Case Western Reserve University, Cleveland, OH 44106, USA
e-mail: bushan@gmail.com;
bushan.k.purushothaman@medtronic.com

Present Address:
B. K. Purushothaman
Medtronic, Mounds View North Facility, 8200 Coral Sea Street NE, MVN51, Mounds View, MN 55112, USA

Martin and Morrison [7] developed an ATR spectroelectrochemical system which, for the optically transparent electrode (OTE), used a thin wafer pressed onto an internal reflection prism. Using this design, the number of materials that could be used as OTEs is expanded and disposable OTEs are possible; in their case, a boron-doped diamond film on a thin silicon wafer served as an OTE in the infrared (the underlying silicon is opaque at wavelengths <1 μm). For highly resistive electrolytes, (e.g., lubricants), a lightly-doped thin silicon wafer has sufficient conductivity to serve as the OTE; the thin silicon wafer is more flexible than when diamond-coated, making cell assembly easier. The infrared transparency of the silicon wafer is also higher than the diamond coated wafer yielding higher detection levels of species in the electrolytes. Researchers have used silicon and other semiconductor multi-reflection ATR prisms as OTE's to primarily study semiconductor/electrolyte interfaces [8] and to understand its surface interactions with different electrolytes [9–17]. Silicon (*p*-doped) electrodes have also monitored the growth of electronically conducting polymers [18, 19].

Electrochemical techniques like electrochemical impedance spectroscopy (EIS) and cyclic voltammetry (CV) have demonstrated enormous potential to investigate complex non-aqueous systems like lubricants [20–22]. EIS has monitored variations in the concentrations of detergents, surfactants and dispersants in lubricating oils. Although this method provides a variety of qualitative and quantitative information about the lubricant, EIS lacks detailed chemically-specific information. In addition, many species that form during the ageing of the lubricant can impede the interpretation of the EIS data. A second complementary technique like CV has been used along with the EIS to improve identification of the various components of a typical industrial lubricant.

In contrast to electrochemical techniques, infrared (IR) methods provide specific information on the character of species found in the lubricants. Researchers have shown that in situ Fourier transform infrared (FTIR) spectroscopy provides an excellent qualitative fingerprint of these species [23, 24], including industrially relevant parameters like total acid number (TAN) [25], total base number (TBN) [26], and moisture content [27]. TAN is the amount of potassium hydroxide (KOH) in milligrams that is needed to neutralize the carboxylic acids in one gram of oil and corresponds to the extent of hydrocarbon oxidation in the lubricants. TBN represents the overall lubricant's alkalinity contributed by the additive package in milligrams of KOH per gram of oil. However, validity and interpretation of the results from these methods is often ambiguous.

A powerful tool capable of in situ detection and monitoring of oil additives, surfactants and dispersants and investigation of general mechanisms of oil degradation in an operating engine is of paramount importance for lubricant quality and service life. The combination of in situ ATR–FTIR analysis with electrochemical polarization gives ample spectral width to study a variety of adsorbed or reacted species within electrolytes. By coupling the in situ ATR–FTIR with EIS, a wealth of information about the different species in the lubricants can be obtained as a function of the applied DC potential and oil degradation time. This spectroelectrochemical method has great potential for study of ageing of engine oils and to characterize new lubricants. In this paper, we present the study of lubricant degradation by a combination of EIS and in situ infrared ATR spectroelectrochemistry using boron-doped silicon as the optically transparent electrode. To our knowledge, this paper presents the first attempt to couple IR spectroscopy and EIS simultaneously to study degradation of engine oils.

2 Experimental

The ATR spectroelectrochemical cell developed by Martin and Morrison [7] used a conductive diamond film deposited onto a thin silicon wafer as the optically transparent electrode. The diamond electrode was sandwiched between an ATR cell filled with the electrolyte of interest and a ZnSe prism (single reflection ATR, Harrick Scientific). Proper optical contact must be maintained between the wafer and the ZnSe prism such that IR spectra could be measured at the diamond–liquid interface; this required an electrochemical cell that applied pressure to the wafer uniformly, pressing it onto the ZnSe prism. Best optical contact was achieved when pressure was applied to the electrolyte above the wafer.

For the present work, an improved ATR cell was designed, Fig. 1, which uses hydrostatic pressure to pressurize the cell via screw compression. A boron doped silicon wafer (diameter 1.7 cm, 50 μm thickness, 4–10 Ω cm resistivity, 20 Å thick native oxide, Virginia Semiconductor) is the working electrode and forms the bottom of the electrochemical cell; an o-ring hermetically sealed with vacuum grease serves as the wall of the cell and a stainless steel 316 plate forms the cover and serves as the counter electrode and reference electrode. This ATR cell construction minimized the amount of electrolyte volume thereby reducing the resistance of the lubricant across the electrodes. For electrochemical characterization of lubricants, a highly resistive non-aqueous colloidal system, a two-electrode probe system is more reliable than a four electrode probe system [28]. When a four-electrode probe system is employed, the impedance load, geometry and positioning of voltage electrodes; finite resistance of the impedance analyzer; and capacitive coupling between the signal lines introduced two different types of impedance measurement artifacts. In order to eliminate these artifacts, a two-electrode probe system was utilized in this study.

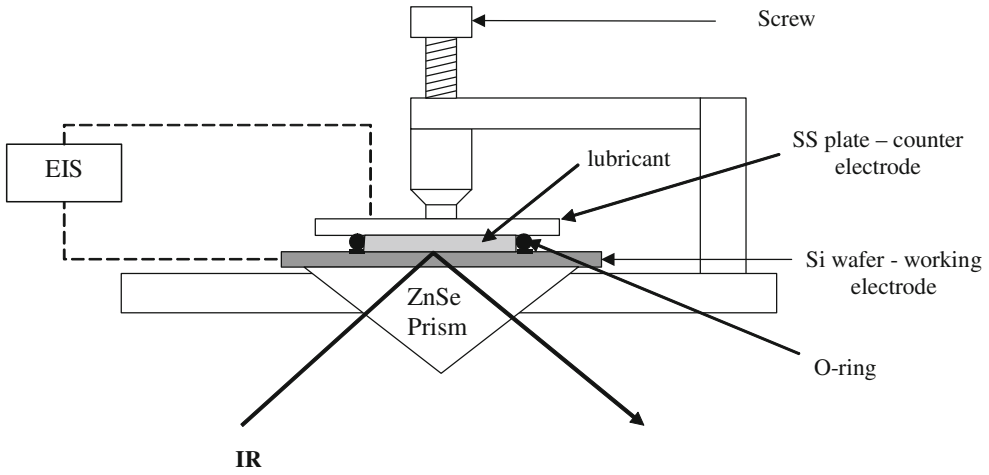

Fig. 1 ATR spectroelectrochemical cell where a plate applies pressure on the o-ring filled with fluid

Prior to cell assembly, the silicon wafer is cleaned with hexane and methanol, and then positioned over the ZnSe prism. The o-ring is then placed onto the wafer, completely filled with fluid, and covered with the metal plate. Pressure to the entire cell is applied by tightening the screw, establishing a liquid-tight seal of the cell and good optical contact between the silicon surface and the ZnSe prism. IR light enters through the ZnSe prism normally, then through the silicon wafer at an incident angle of 45° and is then totally internally reflected, with the incident angle of 36.9°, at the silicon–fluid interface (silicon–water critical angle = 23°) calculated based on Snell's law of refraction and refractive indices of ZnSe (2.89), silicon (3.42) and water (1.33). Infrared (ATR) spectra were obtained using a Nicolet FTIR spectrometer at a resolution of 8 cm^{-1}, room temperature (25°C) and averaging over 600 scans. Infrared spectra of a select engine oil measured under various pressures in the ATR cell ratioed to the IR spectrum of the ATR cell without the engine oil is shown in Fig. 2. The intensity of the IR features increases with the pressure applied by tightening the screw. Spectral analysis shows that the vacuum grease used as seal is insignificant and does not interfere with the peaks of the engine oil.

Infrared spectra were measured while the cell was polarized using electrochemical impedance spectroscopy (500 mV AC voltage amplitude, 100 kHz to 10 mHz frequency range) with an offset DC voltage (0–9 V versus counter electrode). These experiments were conducted on Voltalab PGZ-402 potentiostat (Radiometer Analytical, Westlake, OH). All oil samples originated from the same passenger car (Buick) engine test at Lubrizol Corporation, were collected every 10 h over the test duration (60 h) and submitted for the EIS–ATR IR analysis. These samples were used to make a direct comparison of a fresh lubricant

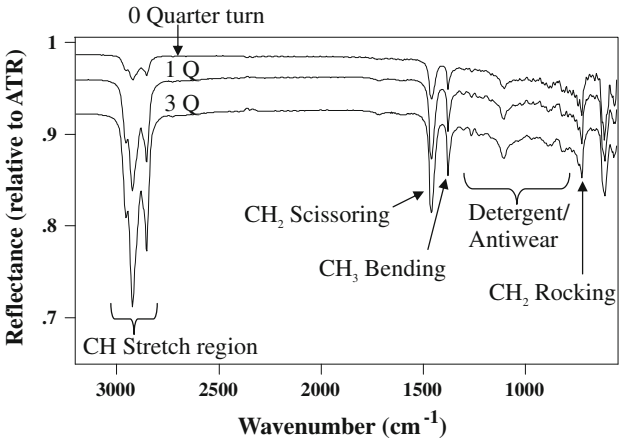

Fig. 2 ATR spectra of 50 h drain oil in the spectroelectrochemical cell. The intensity of the IR features increases with pressure applied using the screw. The different IR features of the hydrocarbon are evident. The IR features of the detergent/antiwear are observed in the wavenumber range 1260–750 cm^{-1}

with that of the spent lubricants. In addition, blends of base oil with individual detergents were prepared and analyzed. A fresh clean silicon wafer was used for each oil sample and EIS–ATR IR analysis.

3 Results and discussion

Industrial lubricants are a complex combination of base oils and performance-enhancing additives designed to improve long-term stability and enhanced performance in aggressive environments [29]. The specialized additives are categorized as detergents, dispersants, oxygen inhibitors, viscosity modifiers and anti-wear agents. These additives are usually present in amounts between 1 and

5 wt% and are composed of a polar functional group and long non-polar hydrocarbon tail that allows the additives to become compatible with the non-polar base oil. Many of these additives are surface active and adsorb onto metal surfaces. The main functions of the detergents are to protect the metal surfaces by film formation and to neutralize the acid products of combustion and thermo-oxidation [22]. The anti-wear agents also form a protective film on the metal surface to decrease wear and tear. Dispersants scatter products such as soot in the bulk of lubricants by a mechanism of association. The oxygen inhibitors minimize the lubricant's oxidation rate [30]. This work focuses on characterization of (a) blends that contain base oil and one type of additive, standard detergents, and (b) fully-formulated passenger car motor oils (lubricants) containing multiple additives. Detergents and anti-wear agents will be analyzed because they are surface active, and our ATR-IR and impedance measurements primarily probe the electrode surface.

3.1 Infrared transmittance characterization of lubricants containing detergents

Initially, FTIR transmittance measurements of pure 'base oil' and 'base oil with detergent' were made, to identify the characteristic IR features for later comparison with ATR cell spectra. 'Base oil with detergent' contained four different detergents, A–D as listed in Table 1. Measurements were also made of concentrated detergents, these samples corresponding to a high concentration (>10%) of detergent in base oil and not the pure detergent. The transmittance of the oils was measured by spreading the oil on a KBr crystal placed in the IR light path.

In the transmittance spectra of 'base oil' and 'base oil with detergent,' IR features for the different CH_x groups in the oil were clearly observed; Table 2 lists the peaks assignments for the C–H bands for the methyl (CH_3) and methylene (CH_2) groups. The C–C stretching vibrations are normally weak and were absent in the measured transmittance spectra. The symmetrical C–H stretching of the methyl group was not visible at the experimentally chosen resolution for the IR measurements as it overlaps with the symmetrical C–H stretching of the methylene group. Similarly, the asymmetrical C–H bending of the methyl group generally overlaps the C–H scissoring vibration of the methylene groups. Additionally, IR features in the 1200–800 cm^{-1} region corresponding to that of the detergent was observed for the 'base oil with detergent'.

Table 1 Composition of the base oil containing detergent

Detergent	Detergent (wt%)	Type
A	1.20	Over-based calcium salt of sulphonic acid
B	1.63	Over-based calcium salt of sulphonic acid
C	0.99	Coupled phenate
D	0.54	Coupled phenate

Table 2 Identification of different hydrocarbon peaks from the transmittance spectra of base oil

Absorption peaks (cm^{-1})	Vibrations
2952	Asymmetrical C–H stretching of CH_3
1375	Symmetrical bending of CH_3
2924	Asymmetrical C–H stretching of CH_2
2854	Symmetrical C–H stretching of CH_2
1460	Scissoring of CH_2
722	Rocking of CH_2

Detergents for use in base oil consist of a polar functional group and a non-polar hydrocarbon tail to make them soluble in the non-polar base oil; the result is an inverse micelle structure. Detergents A and B, shown in Fig. 3a, are calcium carbonate micelles surrounded and stabilized by a calcium salt of sulphonic acid ($SO_3Ca_{1/2}$) [31]. These two detergents differ by the number of calcium carbonate molecules in the micelle (6 and 1.5, respectively). Figure 4 shows IR spectra of concentrated detergents A and B; for detergent A, bands at 1183 and 1047 cm^{-1} are assigned respectively to the asymmetric and symmetric stretching of SO_2 group. Similarly, for detergent B, the bands are at 1192 and 1052 cm^{-1}. This assignment is consistent with literature; anhydrous sulphonic acids display the SO_2

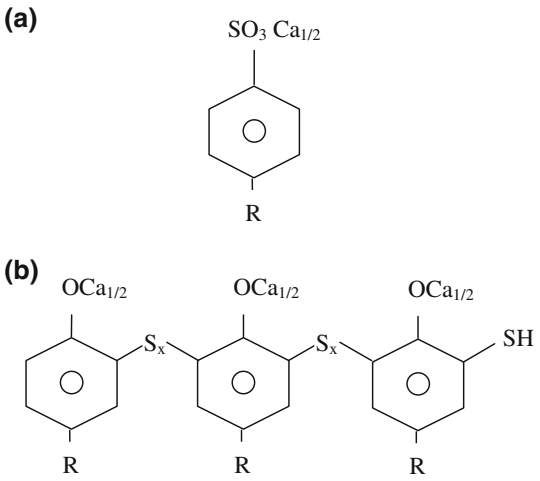

Fig. 3 Structure of different detergents: **a** Structure of sulfonate salt in detergent A and B. R is an alkane containing 20–24 carbons. **b** Structure of coupled phenate (surfactant) in detergent C and D. R is an alkane containing 12 carbons

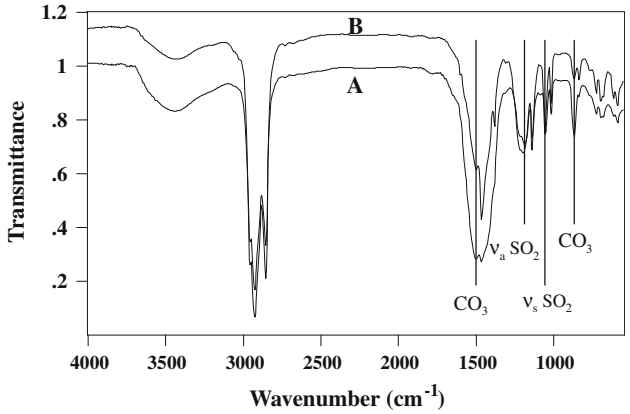

Fig. 4 Transmittance spectrum of detergents A and B. Peaks at 1495 and 863/864 (spectrum A/B) cm^{-1} are characteristic of the carbonate group while peaks at 1183/1192 (spectrum A/B) and 1047/1052 cm^{-1} (spectrum A/B) are characteristic of the SO_2 group

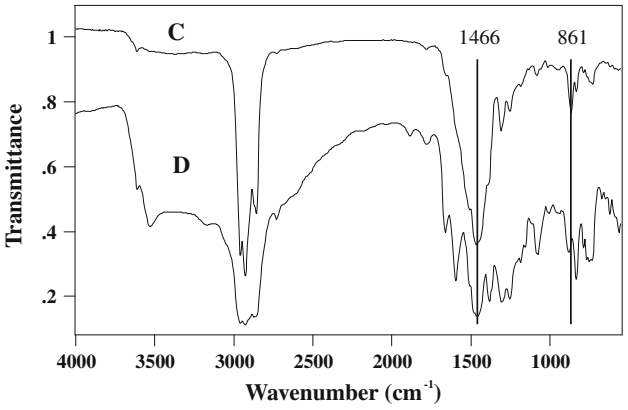

Fig. 5 Transmittance of detergents C and D. The peaks near 3000, 1460, 1375, and 722 cm^{-1} correspond to CH_2 and CH_3 group vibrations. The broad peak at 1466 cm^{-1} is the phenate band. The peak at 861 cm^{-1} is a signature of the carbonate group

stretching bands [32, 33] near 1350 and 1170 cm^{-1}. In contrast, the SO_2 stretching bands for metallic sulphonates [33] differ considerably, near 1190 and 1050 cm^{-1}. For both detergents, a band at 863/864 cm^{-1} is assigned to the C=O bending of calcium carbonate; the peak intensity is smaller for detergent B than for detergent A, as expected, because micelles in detergent B contain less $CaCO_3$ than in detergent A. Another asymmetric stretching band, C=O, from carbonate at 1495 cm^{-1} overlaps with scissoring band of the methylene group of the hydrocarbons and serves as a clear marker to distinguish between the base oil and the detergent.

Detergents C and D are phenate systems in which the calcium carbonate dispersions are stabilized by an aryl sulphonic acid (Fig. 3b). The surfactant anion is a bidentate ligand consisting of a sulfur-bridged phenate. Figure 5 shows IR spectra of these two detergents. The broad intense band at 1466 cm^{-1} corresponds to that of the phenate group [34] while the bands at 1493 and 862 cm^{-1} represent the vibrations of the carbonate peak, consistent with the other detergents. Characteristic peaks for the O–H stretch and bend of the alkyl phenol (3339 and 1241 cm^{-1}) are absent in the phenate detergents [34]. Other remaining peaks were not labeled to keep the complexity to a minimum.

3.2 Spectroelectrochemical ATR characterization of lubricants with detergents

Figure 6 shows the C–H stretch region (3000–2800 cm^{-1}) of the IR spectrum of the 'base oil' and 'base oil with detergent' measured in situ while polarizing the cell. These ATR spectra polarized to different DC voltages are ratioed spectra; i.e., the sample spectrum at each voltage is ratioed to the background spectrum at 0 V, thus providing a

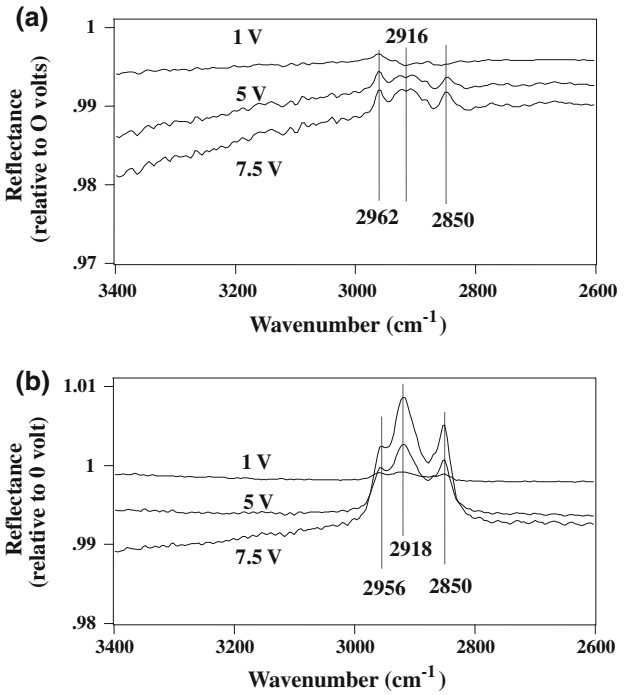

Fig. 6 IR spectra of the base oil (**a**) and base oil with detergents (**b**) in 3000 cm^{-1} region at various electrochemical potentials. Depletion of hydrocarbons containing methyl and methylene groups is observed as the spectro-electrochemical cell is polarized to higher anodic potentials. All spectra are ratioed to the spectrum at 0 V

relative measure of the change in absorbance. It is noted that the IR spectra are offset in Fig. 6 to clearly show the spectral changes at different voltages. The methyl and methylene peaks for the base oil are visible (Fig. 6a) and change with the applied potential. These spectral changes with potential are not due to the evanescent wave path length changes in silicon wafer because the applied potential is mostly spent on the lubricants due to the five

orders of magnitude higher electrolyte resistance in comparison to that of the silicon electronic resistance. An increase in reflectance, which corresponds to a decrease in IR absorbance (upward peak), is consistent with a smaller hydrocarbon concentration near or physisorbed to the silicon electrode surface; correspondingly, a decrease in IR reflectance, which corresponds to an increase in IR absorbance (downward peak), means increased concentration. Thus, the spectra (Fig. 6a) indicate that the hydrocarbon concentration near or physisorbed to the electrode decreases as the cell potential is increased. Two possible mechanisms can account for the change in the peak intensity. Physisorbed hydrocarbon containing species could be electrostatically repelled by the applied potential, decreasing the hydrocarbon at the silicon electrode surface. Alternatively, the hydrocarbons may be depleted by oxidation at the silicon electrode. However, it takes many weeks of operating at temperatures greater than 100°C plus sheer/truncating lubricants to get a sizeable oxidation [35]. In our case, oxidation is negligible as measurements were performed at room temperatures, and kinetics rate constant of charge transfer are very low even at higher potentials [20]. We have what is often referred to as "interfacial polarization" typical for ionic solutions—by increasing potential we attract or repel more ions to the surface and essentially promote physisorbtion [22]. However these ions practically do not exchange charges with the surface**.** As the cell potential increases (Fig. 6a), there is a larger driving force for the electrostatic repulsion of the hydrocarbon containing species near the silicon electrode. The areas under the peak intensities of different groups represent the concentration of the species adsorbed on the electrode surface and that present in the evanescent path length near the electrode surface. The depth of penetration, d_p, of the evanescent wave is a function of the wavelength (λ) of incident light [2]:

$$d_p = \lambda/(2\pi(\sin^2\theta - (n_2/n_1)^2)^{1/2})$$

where θ is the angle of incidence at the silicon–electrolyte interface, n_2 is the refractive index of the electrolyte (1.33) and n_1 is the refractive index of the silicon wafer (3.42). The penetration depth is about 0.9 and 7.0 μm at 4000 and 500 cm^{-1} wavenumbers for our system and clearly shows that the observed IR spectra is not only due to the species on the electrode surface but also species near the electrode surface. Since we cannot currently distinguish between changes at the surface and in the near-electrode region, for the remainder of our discussion, we will refer to these combined concentrations as "local concentrations".

For the 'base oil with detergent,' the C–H stretch peak intensities for the methyl and methylene groups (Fig. 6b) also increase as the potential is increased, presumably due to the same surface depletion as that of the 'base oil' (no detergent, Fig. 6a). Differences in the peak intensities are observed when comparing the 5.0 and 7.5 V polarized 'base oil' spectra and their detergent-containing counterpart (Fig. 6a, b); these changes are consistent with the 'base oil with detergent' depleting hydrocarbons more strongly from the solution near the silicon electrode than the 'base oil'. The hydrocarbon is displaced by detergent at the electrode surface as the detergent performs its primary function of film formation (adsorption) onto the metallic surface [29].

Electrochemical impedance spectroscopy (EIS) was obtained simultaneously with the IR spectra. The Nyquist plot representing real impedance and imaginary impedance along x and y axis respectively for 'base oil with detergent' is shown in Fig. 7. An in-depth analysis of EIS of industrial lubricants at 120 °C has been published elsewhere [22]. In that analysis, an equivalent circuit model was developed based on analysis of the lubricant impedance spectra over the AC frequency range (10 MHz to 1 mHz). According to the model, the bulk resistance, R_{bulk}, in the whole high frequency region (10 MHz to 10 Hz) was identified as being representative of processes occurring in the bulk solution of lubricants, a non-aqueous colloidal system. The bulk resistance and capacitance is associated with orientational polarization of free dipoles of individual additives and relaxation process related to inverse micelles and their aggregates or "macro-ions". The bulk resistance, R_{bulk}, is dependent on the concentration of charge carrying components, their types, the system temperature, the age of oil and the geometry of the testing cell. However, it does not dependent on the applied potential. The faradaic processes including the charge transfer resistance, R_{ct}, is represented in the low frequency region (10 Hz to 1 mHz). The charge transfer resistance follows the Butler–Volmer relationship and therefore decreases with increase in the applied potential. At high temperatures (>100 °C), the bulk resistance and charge transfer resistance are evident as two

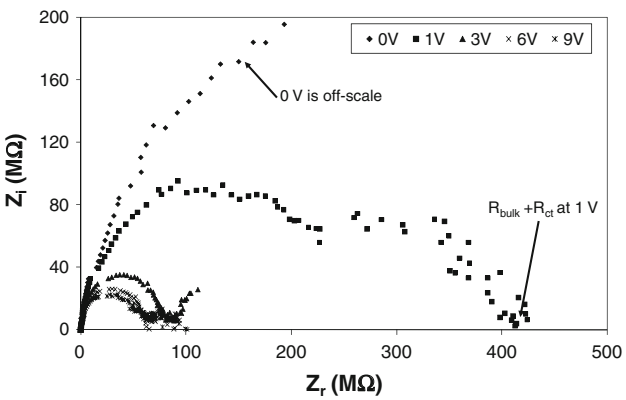

Fig. 7 Impedance spectra of base oil with detergent at different potentials

semi-circles in the EIS spectrum. However at lower temperature such as 25 °C, measurements taken for this analysis, the bulk resistance and charge transfer resistance cannot be resolved and are given as a sum by the diameter of the single depressed semi-circle arc in the EIS spectrum (Nyquist plot). Impedance related to diffusion is also commonly observed in the lower frequency region at higher temperatures, however, the slow diffusion at room temperature is impossible to resolve; therefore, will be not considered further in this analysis.

At 0 V (DC offset potential), the sum of R_{bulk} and R_{ct} is extremely large because of the large impedance for charge transfer (electrochemical reaction) process. However, R_{ct} decreases significantly with increase in the electrochemical potential (0 up to 9 V) typical for charge transfer process, whereas the bulk resistance is unaffected. This results in net decrease in resistance as shown by the decrease in diameter of the semicircle (Fig. 7). The sum of R_{bulk} and R_{ct}, measured for 'base oil with detergent' is about two times smaller than that of the pure 'base oil' at 1 V (figure not shown) due to decrease in bulk resistance. This decrease is because of the presence of detergents in the oil and confirms the inverse relationship between bulk resistance and concentration of polar detergents.

3.3 Study of degradation of fully-formulated lubricants using the ATR cell

ATR–FTIR spectroscopy coupled with EIS spectroscopy was used to study degradation of fully-formulated lubricants containing detergents and anti-wear additives. The main degradation mechanism of the oils is time-dependent oxidation [22]. Industrial oils of different age (fresh, 0, 10, 20, 30, 40, 50 and 60 h) were tested using the ATR spectroelectrochemical cell and ATR–FTIR and EIS spectra were obtained at different potentials. The IR spectra of the 50 h drain oil are shown in Fig. 2. The hydrocarbon peaks corresponding to the CH stretching (methyl and methylene group, 2961, 2925, and 2856 cm^{-1}), the CH_2 scissoring, the CH_3 bending and the CH_2 rocking (values listed in Table 2) are clearly evident.

In Fig. 8 are typical ATR–FTIR ratioed spectra of the 50 h aged drain oil tested at 1, 3, 6, and 9 V; the spectra are ratioed to the relevant spectrum obtained at 0 V. The hydrocarbon peaks corresponding to the CH stretching (methyl and methylene group) are seen, however, the CH_2 scissoring, the CH_3 bending and the CH_2 rocking are not evident in the ratioed spectrum (Fig. 8) as they are overshadowed by the water vapor peaks in the wavenumber range 1980–1350 cm^{-1} and silicon fringes in the wavenumber range 750–550 cm^{-1}. This is because the peak intensities of IR features are significantly smaller in the ratioed spectra (Fig. 8) than in comparison to the original IR spectra (Fig. 2)

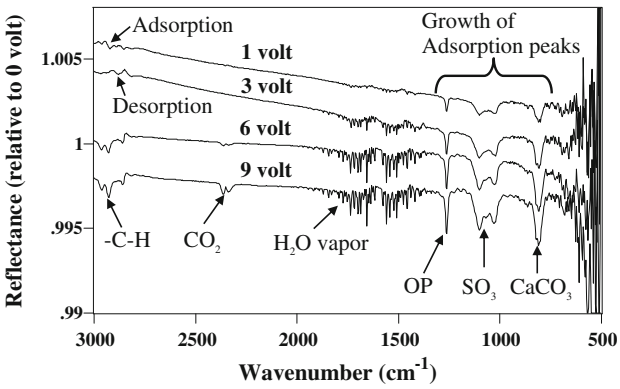

Fig. 8 ATR spectra of 50 h drain oil at different potentials. All spectra are ratioed to 0 V. The intensity of the IR features of different species present in the oil changes with the applied potential

and are therefore affected by small changes in water vapor present in the sample compartment. In addition to the CH stretching features, three major IR features corresponding to the detergent and antiwear additives, that are surface active, are observed between 1260 and 750 cm^{-1} (Figs. 2, 8).

The IR band at 1261 cm^{-1} is assigned to the P=O stretch in the aromatic-O–P structure of zinc dithiophosphate (ZDP) [36], a characteristic functional group in the anti-wear agent. Other peak assignments are the symmetrical stretching of the SO_2 group of the detergents between 1100 and 1024 cm^{-1} (transmittance measurement, Fig. 4) and the C–O bend at 802 cm^{-1} for the detergent's CO_3 group. These peaks were observed in the transmittance spectra of the detergents in Figs. 4 and 5.

Changes with respect to applied potential in the IR features may correspond to adsorption/desorption of species or formation/depletion of species due to reactions at the electrode surface. The hydrocarbon bands (2961, 2925, 2856 cm^{-1}) indicate increased adsorption to the silicon electrode of the hydrocarbon species when electrochemically polarized at 1 V. The spectra predict a reversal to desorption of the hydrocarbon species at 3 V and then back to adsorption for potentials 6 and 9 V. The hydrocarbon peaks evident in the spectrum correspond to the complex mixture of base oil and additives. The reversal of desorption to adsorption with potential is attributed to adsorption of some chemical species and desorption of other chemical species. Also, it is clear from Fig. 8 that the IR absorption of PS, SO_2 and CO_3 groups associated with the additives increases with applied anodic potentials. This suggests an increase in adsorption of ZDP and detergents onto the electrode surface or reaction products with the increase in overpotential. As indicated previously, reaction of a traditional type with electron exchanges are extremely slow, while adsorption is very facile especially at low temperatures and therefore is logical to consider the peak increase is due to adsorption [20, 22].

The IR absorption for given peaks was integrated, each peak area calculated for the IR spectrum collected at a constant DC potential ratioed to 0 V; these are summarized for different aged drain oils in Fig. 9. Positive values for a peak area (Fig. 9) correspond to larger local concentration (more adsorption) and negative values correspond to smaller local concentration (more desorption) of the species in the solution near the electrode surface as compared to the same oil at 0 V. Figure 9a shows the area under the IR peak (1260 cm^{-1}) assigned to the aromatic-O–P structure of ZDP as function of oil drain time and potential. The area for the symmetrical stretching band of the SO_2 group (1050–1054 cm^{-1}) was calculated by integrating over the 1102–1025 cm^{-1} range and is plotted in Fig. 9b as a function of drain oil time and potential. Figure 9c, d show the areas of the IR feature 820–807 cm^{-1} and the IR feature 2970–2850 cm^{-1} assigned to the CO_3 group of the detergent and to the hydrocarbons, respectively.

The peak areas in Fig. 9 corresponding to the IR features of the OP, SO_2 and CO_3 group are maxima for the 30 h drain oil and are significantly smaller for other drain oils. This indicates that adsorption of ZDP and detergents on the silicon surface are a maximum for the 30 h drain oil. This maximum represents the stage at which the oil degradation accelerates and thus is an indicator of lubricant stability. The areas of the IR features (OP, SO_2 and CO_3) of the different drain oils increase monotonously with applied potential, suggestive that higher potentials lead to increased adsorption of ZDP and detergents. In contrast, Fig. 9d shows no definite trend for the change in hydrocarbon feature intensity, with two maxima visible for 0 and 30 h drain oils. As indicated before, the hydrocarbon peaks in the infrared spectra correspond to a complex mixture of species adsorbing and desorbing from the silicon surface for different aged oils. This shows that hydrocarbon adsorption for oils have no correlation with detergent adsorption. A transition from adsorption to desorption of hydrocarbon peaks is evident from the 50 h to the 60 h drain oil. This behavior correlates with complete deterioration of the engine oil at 60 h, as can be concurred by visual inspection of the discolored oil.

Impedance spectra obtained at different DC potentials for different oil drain times were analyzed to obtain the sum of bulk resistance, R_{bulk}, and charge transfer resistance, R_{ct}, of the oil (Fig. 10). For different drain oils, the total resistance decreased with increase in potential, because the charge transfer resistance, R_{ct}, decreased with increase in potential although the bulk resistance is unaffected. The decrease in charge transfer resistance is also associated with increase in the concentration of the detergents and other polar additives which facilitate electrochemical reactions. These concentrations increase with

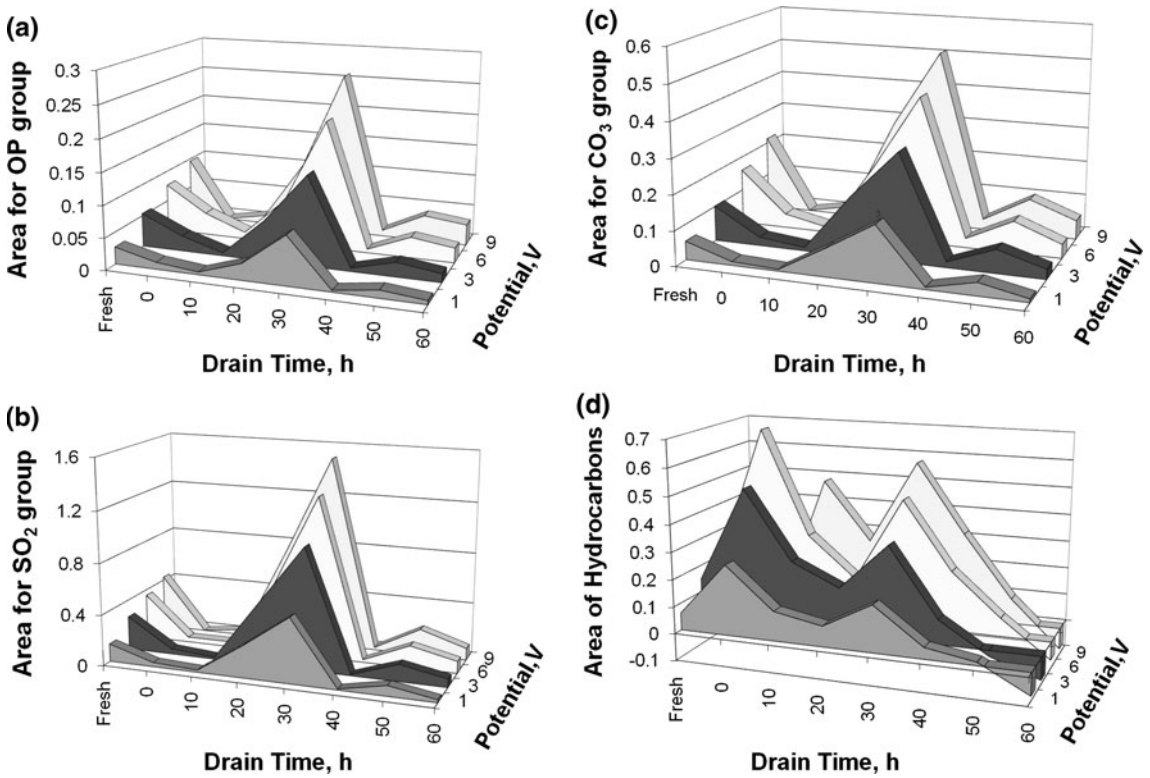

Fig. 9 Area under different IR features corresponding to OP (**a**), SO_2 (**b**), CO_2 (**c**) and hydrocarbons (**d**) for different drain oil times and different potentials. The area of the PO, SO_2 and CO_2 groups are a maximum for the 30 h drain oil and increases with increase in the applied potential

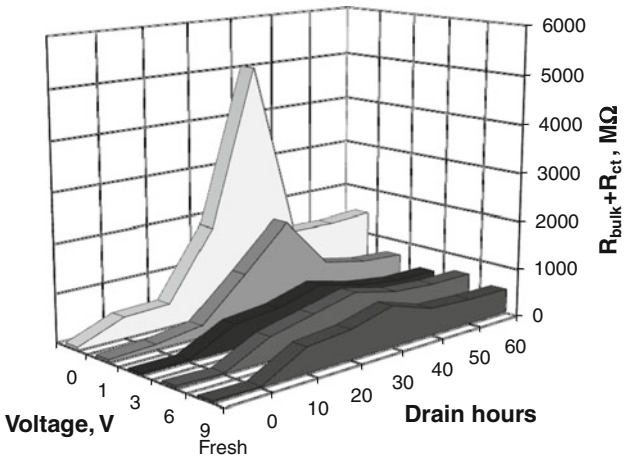

Fig. 10 The sum of bulk and charge transfer resistance as a function of different drain oil times and different potentials. The resistance is a maximum for the 30 h drain oil and decreases with increase in the applied potential

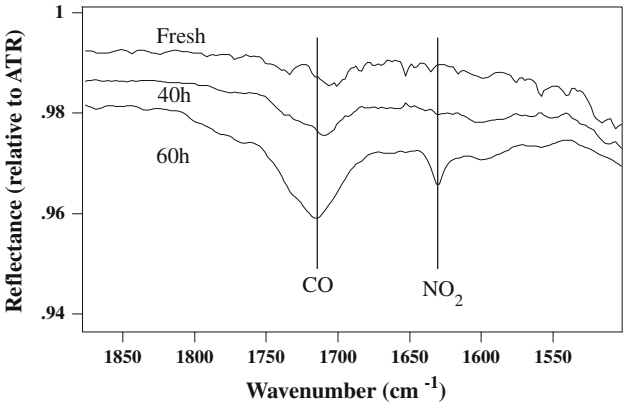

Fig. 11 ATR spectra of fresh, 40 and 60 h drain oil. The oxidation peak (CO) and nitration peak (NO_2) are observed for the 60 h drain oil. However no such peaks are observed for the fresh oil

potential, due to the migration flux of polar detergents and other additives toward the electrode. This is supported by the ATR-IR spectra results which show an increase in the peak areas of the additives with increase in potentials (Fig. 10).

Figure 10 shows that for any applied potential, the sum of R_{bulk} and R_{ct} is at a maximum for the 30 h drain oil. Previous literature [22] indicate that the detergents form superstructures with lower mobility for oils aged to 30 h resulting in increased bulk resistance as confirmed by our EIS results. This also correlates with ATR spectra results showing maximum adsorption of ZDP and other detergents for the 30 h drain oil (Fig. 9). The detergent superstructures break down because of oil oxidation producing more polar mobile species with higher mobility for oils aged to 40, 50 and 60 h resulting in decreased bulk resistance. This sharp decrease in the total resistance, $R_{bulk} + R_{ct}$, for oils greater than 30 h drain time is shown in Fig. 10 and correlates with decrease in the ZDP and other detergent concentration on the silicon electrode (Fig. 9). The EIS data analysis agrees well with the IR spectroscopic trends. To our knowledge, this is the first paper that confirms the degradation of oils by showing the relationship between the detergent superstructures and bulk resistance. This discussion clearly shows that the spectroelectrochemical method provides chemically specific information and offers more informative lubricants' analysis than limited restrictive lubrication laboratory or purely electrochemical techniques.

3.4 ATR characterization of oil degradation products

Figure 11 compares the ATR spectra of fresh oil, 40 and 60 h drain oil without applying any potential. For the 60 h drain oil, two IR features (1630 and 1715 cm^{-1}) are observed corresponding respectively to the nitration and oxidation products of oil degradation (i.e., oxidation) [24]. These IR features are not observed in the fresh oil. This data shows that more polar species are formed at and above 40 h drain oil resulting in decreases bulk resistance and supports the results discussed in the previous section. The IR feature at 1715 cm^{-1} is assigned to the C=O stretch from carboxylic acids, ketones and aldehydes formed by oil oxidation. The IR feature at 1630 cm^{-1} is assigned to both the asymmetric and symmetric stretch of the NO_2 group. The nitration products are formed when there is an excessive advance of the spark in the gasoline engines. These IR features clearly indicate oil degradation; however, the effect of polarization (applied potential) on these IR features could not be observed due to interference by the bands for water vapor as shown in the Fig. 8. In the future, the infrared spectrometer will be purged with inert gas to minimize the presence of the water vapor features.

The surface of the silicon electrode used in ATR cell roughens when in contact with the lubricant [37]. However, the electrode provides sufficient stability to monitor the oil samples for the duration of the EIS measurements. The effect of silicon surface roughening on sensor properties will be studied in the future. Alternatively, diamond deposited on silicon wafers, which is chemically resistant, can be used as the working electrode in the ATR cell. In addition, this spectroelectrochemical method can assist in the development of new additives.

4 Conclusions

An attenuated total reflectance spectroelectrochemical cell was designed using thin silicon wafers in optical contact with a ZnSe prism as the internal reflection element to

study lubricants. The ATR cell construction minimized the electrolyte volume, thereby reducing the electrolyte resistance of the lubricants across the electrodes. Boron-doped silicon wafers served well as disposable, optically transparent electrodes for short-term ATR spectroelectrochemical measurements of resistive electrolytes, especially industrial oils.

Previously, lubricants have been studied separately by electrochemical and IR spectroscopy techniques. Here, we analyzed them simultaneously with electrochemical impedance spectroscopy and ATR-IR spectroscopy. The degradation of lubricants was demonstrated by changes in the IR features corresponding to that of the hydrocarbon, detergent and anti-wear additives at different applied DC potentials. ATR-IR spectral analysis shows that adsorption of the detergents and the anti-wear additives are at a maximum for the 30 h drain oil, and then decrease with older and thus more degraded oil. Similarly, the sum of the bulk resistance, R_{bulk}, and the charge transfer resistance, R_{ct}, calculated from EIS analysis, is at a maximum for the 30 h drain oil. This is due to the formation of detergent superstructures at lower drain times ($\leq$30 h) resulting in increased resistance and subsequent break down of the superstructures into more polar mobile species at longer drain times (>30 h) resulting in decreased resistance. The simultaneous EIS and ATR-IR studies predict degradation of lubricants above 30 h of age. This analysis shows the feasibility of using a silicon wafer OTE in an ATR cell to monitor degradation of oils. The molecular specificity of ATR in combination with controlled electrode–electrolyte interface reactions of electrochemistry is a powerful tool to investigate degradation and formulation of oils.

Acknowledgments This research was supported by Case School of Engineering. Helpful discussions with Prof. John Angus are acknowledged.

References

1. Hind AR, Bhargava SK, McKinnon A (2001) Adv Colloid Interface Sci 93:91
2. Harrick NJ (1967) Internal reflection spectroscopy. John Wiley & Sons, New York
3. Stole SM, Popenoe DD, Porter MD (1991) In: Abruna HD (ed) Electrochemical interfaces: modern techniques for in situ interface characterization. VCH Publishers, New York, p 589
4. Anderson MR, Taylor CD (2000) In: Meyers RA (ed) The encyclopedia of analytical chemistry. John Wiley & Sons, New York, p 9849
5. Hansen WN, Kuwana T, Osteryoung RA (1966) Anal Chem 38:1810
6. Murray RW, Heineman WR, O'Dom GW (1967) Anal Chem 39:1666
7. Martin HB, Morrison PW Jr (2001) Electrochem Solid St 4:E17
8. Chazalviel JN, Fellah S, Ozanam F (2002) J Electroanal Chem 524–525:137
9. DuBois DL, Turner JA (1982) J Am Chem Soc 104:4989
10. Tyagai VA, Gorodyskii AV, Dogonadze RR, Kolbasov GY (1981) Elektrokhimiya 17:314
11. Rao AV, Chazalviel JN, Ozanam F (1986) J Appl Phys 60:696
12. Rao AV, Ozanam F, Chazalviel JN (1990) J Electron Spectrosc 54–55:1215
13. Ozanam F, Djebri A, Chazalviel JN (1996) Electrochim Acta 41:687
14. Fonseca Cd, Ozanam F, Chazalviel JN (1996) Surf Sci 365:1
15. Chazalviel JN, Belaidi A, Safi M, Maroun F, Erne BH, Ozanam F (2000) Electrochim Acta 45:3205
16. Lewerenz HJ (1997) J Phys Chem B 101:2421
17. Kimura Y, Nemoto J, Shinohara M, Niwano M (2003) Phys Status Solidi A 197:577
18. Rangamani AG, McTigue PT, Verity B (1994) Synthetic Met 64:91
19. Fan Q, Ng LM (1996) J Vac Sci Technol A 14:1326
20. Lvovich V, Cahoon J, Riga A (2001) ASTM Spec Tech Publ STP 1402:157
21. Smiechowski MF, Lvovich VF (2002) J Electroanal Chem 534:171
22. Lvovich VF, Smiechowski MF (2006) Electrochim Acta 51:1487
23. Powell JR, Compton DAC (1993) Lubr Eng 49:233
24. Toms AM, Powell JR (1997) P/PM technology, pp 58–64
25. Dong J, Van De Voort FR, Ismail AA, Akochi-Koble E, Pinchuk D (2000) Lubr Eng 56:12
26. Dong J, van de Voort FR, Yaylayan V, Ismail AA, Pinchuk D, Taghizadeh A (2001) Lubr Eng 57:24
27. Dong J, Van de Voort FR, Yaylayan V, Ismail AA, Pinchuk D, Brazeau A (2000) Lubr Eng 56:30
28. Lvovich VF, Smiechowski MF (2009) J Appl Electrochem 39:2439
29. Mortier RM, Orszulik ST (1992) Chemistry and technology of lubricants. Blackie Academic & Professional, London
30. Johnson M, Korcek S, Djensen R, Gangopadhyay A, Soltis E (2001) SAE technical paper 013541
31. Rizvi SQA (1995) Lubricants and lubricant additives. Lubrizol Corp
32. Detoni S, Hadzi D (1957) Spectrochim Acta 11:601
33. Socrates G (2004) Infrared and Raman characteristic group frequencies: tables and charts, 3rd edn. Wiley, Chichester
34. Griffiths JA, Bolton R, Heyes DM, Clint JH, Taylor SE (1995) J Chem Soc Faraday T 91:687
35. Goodlive SA, Lvovich VF, Humphrey BK, Boyle FP (2004) SAE technical paper series 2004-01-3010
36. Aktary M, McDermott MT, Torkelson J (2001) Wear 247:172
37. Pelsozy M (2002) Internal lubrizol document. Lubrizol Corp